Effects of disorder and interactions in the quantum Hall ferromagnet

D. Makogon, A. Alamir, and C. Morais Smith
Institute for Theoretical Physics, University of Utrecht, Leuvenlaan 4, 3584 CE Utrecht, The Netherlands
(Received 23 August 2009; revised manuscript received 5 November 2009; published 12 January 2010)

This work treats the effects of disorder and interactions in a quantum Hall ferromagnet, which is realized in a two-dimensional electron gas (2DEG) in a perpendicular magnetic field at Landau-level filling factor $\nu=1$. We study the problem by projecting the original fermionic Hamiltonian into magnon states, which behave as bosons in the vicinity of the ferromagnetic ground state. The approach permits the reformulation of a strongly interacting model into a noninteracting one. The latter is a nonperturbative scheme that consists in treating the two-particle neutral excitations of the electron system as a bosonic single particle. Indeed, the employment of bosonization facilitates the inclusion of disorder in the study of the system. It has been shown previously that disorder may drive a quantum phase transition in the Hall ferromagnet. However, such studies have been either carried out in the framework of the nonlinear sigma model, as an effective low-energy theory, or included the long-range Coulomb interaction in a quantum description only up to the Hartree-Fock level. Here, we establish the occurrence of a disorder-driven quantum phase transition from a ferromagnetic 2DEG to a spin-glass phase by taking into account interactions between electrons up to the random-phase approximation level in a fully quantum description.

DOI: 10.1103/PhysRevB.81.045310 PACS number(s): 73.43.Nq, 75.10.Nr, 75.30.Ds

I. INTRODUCTION

The simultaneous treatment of disorder and interactions in strongly correlated electron systems has always formed a knotty challenge; this is because of the dearth of manageable analytical techniques that can deal with disorder and interactions at the same time.[1–4] The strongly correlated system of interest in this work is the two-dimensional electron gas (2DEG) in a perpendicular magnetic field at Landau-level filling factor $\nu=1$, whose ground state is commonly known as the *quantum Hall ferromagnet*.

The quantum Hall ferromagnet is the spin-polarized ground state of the 2DEG at $\nu=1$ in which all electrons completely fill the lowest Landau level with spin-up polarization. Such configuration minimizes the Coulomb energy for fermionic systems. In general, it is a competition between kinetic and Coulomb energies, which determines the ground state. In the case of the quantum Hall ferromagnet having $\nu=1$ the kinetic energy is frozen and does not change with spin flip, thus, the ground state is ferromagnetic, even with zero Zeeman splitting. Typically, the Zeeman splitting in the GaAs heterojunctions turns out to be roughly 70 times smaller than the spacing between Landau levels and an order of magnitude smaller than the Coulomb energy per particle.

The neutral elementary excitations are spin-wave excitations, also called magnons. The spin waves can be described by the action of the spin lowering operator $S_{\mathbf{q}}^{-}$, projected to the lowest Landau level, on the ferromagnetic ground state. It turns out, that the projected operator creates an exact excited eigenstate of the Hamiltonian. In the regime of low momenta, the magnon's dispersion is quadratic and the coefficient of the quadratic term represents a phenomenological constant known as the *spin stiffness*. The spin stiffness provides a measure of the free-energy increment associated with twisting the direction of the spins. A significant spin stiffness indicates that the system lies in the ferromagnetic phase, while a paramagnetic state corresponds to a vanishing spin stiffness. The spin-wave dispersion at very large momenta saturates at a constant value given by the sum of the Coulomb and Zeeman energies. Thus, at large momenta, the value corresponds to the energy of separate quasiparticle and quasihole excitations.

One approach that has successfully dealt with strongly correlated electron systems is the so-called *bosonization* procedure. Bosonization is a nonperturbative approximation scheme that essentially treats the electron-hole excitation, known as *exciton*, as a bosonic single particle; consequently, a fermionic Hamiltonian can be recast into a bosonic one. In 1950, Tomonaga revealed, in a ground-breaking paper,[5] that the application of the bosonization formalism to a one-dimensional EG (1DEG) yielded an exactly solvable Hamiltonian. The reason is that the electron and the hole propagate with nearly the same group velocity in the low-energy region. However, that is not the case in two dimensions. At a given momentum k, the particle-hole pair excitation holds a continuous range of energies. Therefore, it is less straightforward to construct a coherently propagating bosonic entity in two dimensions.

The first attempt to extend the bosonization procedure for higher dimensions was done by Luther[6] and then revised by Haldane.[7] Castro Neto and Fradkin,[8] as well as Houghton and Marston,[9,10] developed a bosonization technique for a Fermi liquid in any number of dimensions. As regards the interacting 2DEG subject to an external perpendicular magnetic field, Westfahl Jr. *et al.*[11] constructed a formalism that treated the elementary neutral excitations of the system, the *magnons*, in a bosonic framework such that the fermionic Hamiltonian of the system was transmuted into a quadratic bosonic Hamiltonian. The drawback is that this method is valid in the limit of weak magnetic fields, which amounts to large Landau-level filling factors ν.

Doretto *et al.*[12] extended the methodology of Westfahl Jr. *et al.*[11] to the case of the 2DEG at $\nu=1$ (i.e., for a very strong magnetic field). Given that the system is now restricted to one Landau level, the task greatly simplifies, since the

Landau-level quantum degree of freedom can then be disregarded. Projecting the original fermionic interacting Hamiltonian of the system into the lowest Landau level, which is completely filled ($\nu=1$), allows one to expand it in magnon states.[13] It then turns out remarkably that the dispersion relation of the free magnons coincides with the result derived by Bychkov *et al.*[14] and also by Kallin and Halperin[15] within the fermionic description at the *random-phase approximation* (RPA) level and the quartic interacting part of the magnon Hamiltonian might be related to the skyrmion-antiskyrmion neutral excitations of the Hall ferromagnet.[12] Moreover, in the vicinity of the ground state, without magnon-magnon interactions, magnons behave like bosons. This allows to treat magnons approximately as bosons in the so-called single-mode approximation.[16]

Here, we intend to calculate a quantum phase transition in the quantum Hall ferromagnet driven by disorder, accounting for the Coulomb interactions between electrons. We will use the bosonization technique allied to the usual self-consistent Born approximation for the disorder averaging procedure.

Before presenting the results obtained in this paper, it is worth getting acquainted with the current status of research related to the field. To begin with, Green[1] propounded that the vanishing of the renormalized spin stiffness at a threshold value of the disorder strength signifies the occurrence of a depolarization transition from the ferromagnetic phase to a paramagnetic one. His finding is based on a previous result established by Fogler and Shklovskii,[17] who proffered the same idea in the case of higher Landau levels. Green established this proposition in the framework of nonlinear sigma model, used as an effective low-energy theory in the regime of weak disorder. The other quantity that Green computed is the disorder contribution to the optical conductivity, which he found to be unmeasurably small. Finally, Green established that the quantization of the Hall conductivity is not affected by the presence of weak disorder in the system.[1]

Another work was carried out by Sinova *et al.*,[2] who established the occurrence of a phase transition from the paramagnetic state to the partially polarized ferromagnetic one and then finally to the fully polarized ferromagnetic one as the interaction strength increases relative to the disorder strength. They determined this result by computing the average value of the spin polarization as a function of the interaction strength relative to the disorder strength. Sinova *et al.*[2] did consider Coulomb interactions within the framework of the Hartree-Fock approximation. Moreover, the transition from the paramagnetic phase to the ferromagnetic one was found to take place when the Coulomb energy scale is about twice as large as the Landau-level-broadening disorder energy scale. As a final point, the authors inferred that no phase transition can take place in the strong disorder limit.

A similar problem was considered in the work of Burmistrov,[4] who considered a 2DEG in the weak perpendicular magnetic field with $\nu \gg 1$ and Gaussian distributed disorder. He was able to obtain an effective action for the electrons in the highest Landau level by integrating out the fermionic degrees of freedom of the lower lying Landau levels and making a number of approximations at RPA level. The obtained results show that the presence of disorder weakens the screening from the lower lying Landau levels and thus, leads to an increase in the spin stiffness.

The last germane paper was published by Rapsch *et al.*[3] They established the occurrence of a phase transition from the ferromagnetic state to the so-called spin-glass phase. This result was obtained by calculating the magnetization, the magnetic susceptibility, and the spin stiffness as functions of the disorder strength. They assumed the disorder potential to be Gaussian distributed and described the system in terms of a *semiclassical* spin model. In their model, they took into account Coulomb interactions within the Hartree-Fock approximation but modeled them as being short ranged. Like Green,[1] Rapsch *et al.*[3] computed the disorder contribution to the optical conductivity and found as well that it is undetectable. Finally, they calculated the dielectric susceptibility of both the partially polarized ferromagnetic phase and the spin glass one and they concluded that both regimes display an insulating behavior at low momenta and a metallic behavior at large momenta.

Let us now put our work in perspective. Our objective is to establish the behavior of the renormalized spin stiffness as a function of the disorder strength in order to ascertain a potential quantum phase transition driven by disorder to a nonferromagnetic state. Indeed, if the spin stiffness vanishes for a critical value of the disorder strength, then this signals an instability in the ferromagnetic phase.[1] On the other hand, the appearance of an imaginary component of the spin stiffness, which might be interpreted as a spin-wave damping,[18,19] at a certain disorder strength, might indicate the appearance of localized spin waves and a spin-glass phase transition. Another important characteristic is the Pauli susceptibility, which diverges at the point of the phase transition from a nonferromagnetic to a ferromagnetic state, indicating spontaneous magnetization. We consider a fully *quantum* model, include a short-range weak disorder potential up to the second-order Born approximation and treat the true *long-range Coulomb* interactions up to the RPA level.

The method that we employ consists of five steps. First of all, a bosonized expression of the total Hamiltonian, which includes a contribution from disorder, is sought for. The dispersion relation of the free bosons corresponds to the one computed by MacDonald *et al.*[20] and more explicitly by Doretto *et al.*,[12] which entails interactions between electrons up to the RPA level. The second step consists in obtaining the full Green's function, and precisely its disorder self-average. In our case, because the impurities are randomly distributed throughout the system, the disorder self-average can also be taken by averaging over the impurity positions. The third stage is then to determine the self-energy of that disorder self-averaged Green's function through the use of the Dyson's equation. The self-energy is determined in the low-impurity density and weak-disorder-scattering approximations. As a result, the self-energy corresponds to a single diagram with one propagator line and two disorder potential lines. The propagator line is evaluated within two further possible approximations: the bare approximation, which consists in using the bare bosonic propagator and the self-consistent approximation, which uses instead the full disorder self-averaged Green's function. One must bear in mind that both propagators take into account interactions between electrons up to the RPA level. Furthermore, the bare approxi-

mation is first taken in the long wavelength limit, which keeps the lowest order terms in momenta, and then in the general case, where all the momenta terms are taken into account. The fourth step consists in obtaining the renormalized dispersion in these approximations: bare and self-consistent approximations. The final stage is then to determine the spin stiffness in the approximations by taking the coefficient of the quadratic term in the renormalized dispersion. It is found that a naive extrapolation of the bare approximation to the regime of finite disorder strength predicts vanishing of the renormalized spin stiffness at a certain disorder strength u_p, indicating a paramagnetic phase transition. A more realistic self-consistent approximation, however, predicts even faster decrease in the renormalized spin stiffness with growing disorder strength up to a certain critical value u_c of the disorder. At this point, the renormalized spin stiffness drastically changes its behavior: it becomes nonanalytic, acquires an imaginary part, and the real part saturates at a certain positive value without reaching zero. Such nonanalytic behavior cannot be accessed by any finite number of perturbative corrections. In addition, our calculations show a strong indication that the Pauli susceptibility also diverges at the same critical point u_c, suggesting a phase transition, presumably to a spin-glass phase.

The outline of this paper is the following. In Sec. II we present the model and in Sec. III we derive the expression for the self-energy. Then, we first solve the problem using the bare Green's function in Sec. IV. We present our numerical and analytical results for the self-consistent solution of the Dyson equations in Sec. V and draw our conclusions in Sec. VI.

II. MODEL

The 2DEG in the presence of both a perpendicular magnetic field ($\mathbf{B}=B\hat{z}$) at $\nu=1$ and disorder is described by the fermionic Hamiltonian $\mathcal{H}=\mathcal{H}_0+\mathcal{H}_{\text{imp}}$, with

$$\mathcal{H}_0 = \frac{1}{2m^*}\int d\mathbf{r}\Psi^\dagger(\mathbf{r})[-i\hbar\nabla + e\mathbf{A}(\mathbf{r})]^2\Psi(\mathbf{r}) - \frac{1}{2}g^*\mu_B B\sum_\sigma \int d\mathbf{r}\sigma\Psi^\dagger(\mathbf{r})\Psi(\mathbf{r}) + \frac{1}{2}\sum_{\sigma,\sigma'}\int d\mathbf{r}d\mathbf{r}'\Psi^\dagger_\sigma(\mathbf{r})\Psi^\dagger_{\sigma'}(\mathbf{r}')V(|\mathbf{r}-\mathbf{r}'|)\Psi_{\sigma'}(\mathbf{r}')\Psi_\sigma(\mathbf{r})$$

and

$$\mathcal{H}_{\text{imp}} = \int d\mathbf{r}\sum_{i=1}^{N_{\text{imp}}} U(\mathbf{r}-\mathbf{X}_i)\Psi^\dagger(\mathbf{r})\Psi(\mathbf{r}).$$

Here, $\Psi^\dagger(\mathbf{r})$ and $\Psi(\mathbf{r})$ are, respectively, the fermionic creation and annihilation operators in coordinate space, m^* denotes the effective mass of the electron, $\mathbf{A}$ is the vector potential, g^* stands for the effective Landé g factor, and μ_B is the Bohr magneton. In addition, $V(|\mathbf{r}|)=e^2/(\epsilon|\mathbf{r}|)$ denotes the Coulomb potential, with ϵ being the dielectric constant of the host semiconductor and U stands for the impurity potential, with X_i being the random position of an impurity.

The first step consists in obtaining a second quantized version of the magnon Hamiltonian of the system. In our model we consider only single magnon processes, which allow us to use a bosonic description. It was shown in Ref. 12 that the bosonized Hamiltonian of the system in the absence of disorder is (neglecting a constant term)

$$\mathcal{H}_0 = \sum_{\mathbf{q}} \omega_{\mathbf{q}} b^\dagger_{\mathbf{q}} b_{\mathbf{q}}, \tag{1}$$

where $b^\dagger_{\mathbf{q}}$ and $b_{\mathbf{q}}$ are, respectively, the bosonic creation and annihilation operators in $\mathbf{q}$ space and the bosonic dispersion relation is given by

$$\omega_{\mathbf{q}} = g + \epsilon_B\left[1 - e^{-|\ell\mathbf{q}|^2/4} I_0\left(\frac{|\ell\mathbf{q}|^2}{4}\right)\right]. \tag{2}$$

Here, $\epsilon_B=\sqrt{\pi/2}(e^2/\epsilon\ell)$ stands for the Coulomb energy scale (ℓ being the magnetic length), I_0 denotes the modified Bessel function of the first kind, and $g=g^*\mu_B B$. It must be stressed that although the interaction between magnons is omitted from the discussion, the Coulomb interaction between electrons up to RPA level is taken into account by the bosonic dispersion relation $\omega_{\mathbf{q}}$.[14,15] Moreover, it was shown in Ref. 15 that by taking into account bubble (RPA) and ladder diagrams, one can reproduce the excitation energy exactly in first order of the ratio $\epsilon_B/\hbar\omega_c$ (Coulomb to cyclotron energy) and that all the other diagrams have higher order contributions. Therefore, as long as $\epsilon_B/\hbar\omega_c$ is a small parameter, the use of the RPA approximation (also taking into account the ladder diagrams) is justified.

We now focus on the impurity part of the Hamiltonian. We begin with the fermionic expression of the second quantized impurity Hamiltonian,

$$\mathcal{H}_{\text{imp}} = \sum_{\mathbf{q}} U(\mathbf{q}) g_{\mathbf{q}} \sum_{\mathbf{p}} a^\dagger_{\mathbf{p}+\mathbf{q}} a_{\mathbf{p}}. \tag{3}$$

Here, $g_{\mathbf{q}}$ denotes the Fourier-transformed density function $\Sigma_{j=1}^{N_{\text{imp}}}\delta(\mathbf{x}-\mathbf{X}_j)$ for the impurities and $a^\dagger_{\mathbf{q}}$ and $a_{\mathbf{q}}$ are, respectively, the fermionic creation and annihilation operators in $\mathbf{q}$ space. In order to obtain the bosonic form of the above, the Fourier-transformed electronic density operator must be used. It is given by

$$\rho(\mathbf{q}) = \int d\mathbf{r} e^{-i\mathbf{q}\cdot\mathbf{r}}\Psi^\dagger(\mathbf{r})\Psi(\mathbf{r}). \tag{4}$$

The electronic field operators are related to the single-electron operators by

$$\Psi(\mathbf{r}) = \sum_{\mathbf{p}} \frac{e^{-i\mathbf{p}\cdot\mathbf{r}}}{\sqrt{A}} a_{\mathbf{p}} \quad \text{and} \quad \Psi^\dagger(\mathbf{r}) = \sum_{\mathbf{p}} \frac{e^{i\mathbf{p}\cdot\mathbf{r}}}{\sqrt{A}} a^\dagger_{\mathbf{p}},$$

where A is the area of the system. Substituting the above back into Eq. (4) and then into Eq. (3) yields

$$\mathcal{H}_{\text{imp}} = \sum_{\mathbf{q}} U(\mathbf{q}) g_{\mathbf{q}} \rho(\mathbf{q}). \tag{5}$$

The bosonized version of the electron density operator reads[12]

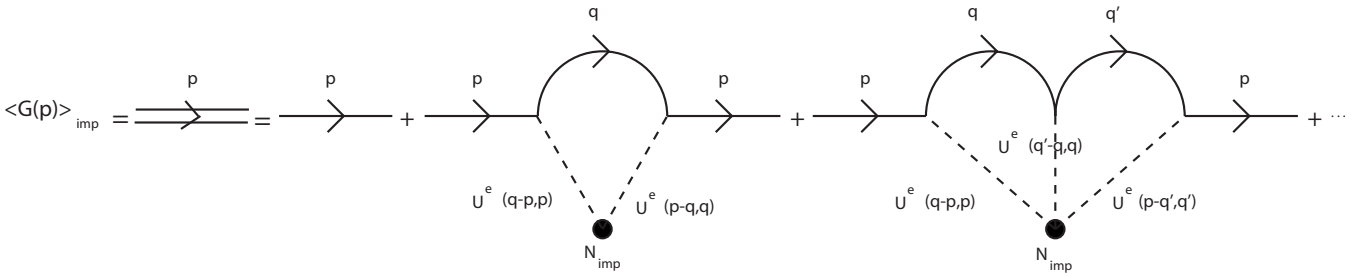

FIG. 1. Diagrammatic expansion of the disorder averaged Green's function.

$$\rho(\mathbf{q}) = \delta_{\mathbf{q},0} N_\phi + 2ie^{-|\ell\mathbf{q}|^2/4} \sum_{\mathbf{p}} \sin\left(\frac{\mathbf{q}\wedge\mathbf{p}}{2}\right) b^\dagger_{\mathbf{q}+\mathbf{p}} b_{\mathbf{p}}, \tag{6}$$

where $N_\phi = A/(2\pi l^2)$ is the Landau-level degeneracy and $\mathbf{q}\wedge\mathbf{p} = \ell^2 \hat{z}\cdot(\mathbf{q}\times\mathbf{p})$. The disorder Hamiltonian then becomes

$$\mathcal{H}_{\text{imp}} = \sum_{\mathbf{q}} U(\mathbf{q}) g_{\mathbf{q}} \Bigg[\delta_{\mathbf{q},0} N_\phi + 2ie^{-|\ell\mathbf{q}|^2/4} \times \sum_{\mathbf{p}} \sin\left(\frac{\mathbf{q}\wedge\mathbf{p}}{2}\right) b^\dagger_{\mathbf{q}+\mathbf{p}} b_{\mathbf{p}} \Bigg]. \tag{7}$$

The constant term $\delta_{\mathbf{q},0} N_\phi$ is now omitted since the quantity of interest is the Green's function.

The bosonized impurity Hamiltonian is then finally written as

$$\mathcal{H}_{\text{imp}} = \sum_{\mathbf{q},\mathbf{p}} U(\mathbf{q}) g_{\mathbf{q}} f(\mathbf{q},\mathbf{p}) b^\dagger_{\mathbf{q}+\mathbf{p}} b_{\mathbf{p}}, \tag{8}$$

where

$$f(\mathbf{q},\mathbf{p}) = 2ie^{-|\ell\mathbf{q}|^2/4} \sin\left(\frac{\mathbf{q}\wedge\mathbf{p}}{2}\right). \tag{9}$$

Labeling

$$U(\mathbf{q}) f(\mathbf{q},\mathbf{p}) = U^e(\mathbf{q},\mathbf{p}), \tag{10}$$

the full bosonized Hamiltonian of the quantum Hall ferromagnet in the presence of impurities is then expressed as

$$\mathcal{H} = \sum_{\mathbf{q}} \omega_{\mathbf{q}} b^\dagger_{\mathbf{q}} b_{\mathbf{q}} + \sum_{\mathbf{q},\mathbf{p}} U^e(\mathbf{q},\mathbf{p}) g_{\mathbf{q}} b^\dagger_{\mathbf{q}+\mathbf{p}} b_{\mathbf{p}}. \tag{11}$$

Let us now say a few words on the dimensions of the disorder potential. There are two sources of disorder present in the system: impurities positioned at a certain distance away from the 2DEG and impurities present in the 2DEG. In the case of GaAs heterostructures,[1,21] most of the disorder potential is spawned by the Coulomb interaction between the electrons and the impurities located away from the 2DEG. These impurities correspond to ionized donor atoms situated in the n-type region, which itself is detached from the 2DEG by an insulating layer of thickness $d \sim 1000$ Å $\gg \ell$. In the present calculations, the disorder potential will be taken as an effective two-dimensional potential.

Having obtained the bosonized Hamiltonian in the presence of impurities, one is now able to determine the expression for the self-energy.

III. DERIVATION OF THE SELF-ENERGY

In the same spirit as Ref. 22, one first looks for the Green's function,

$$G(\mathbf{p}',\mathbf{p};t) = -i\langle 0|T[b_{\mathbf{p}}(t) b^\dagger_{\mathbf{p}'}(0)]|0\rangle. \tag{12}$$

Here, $|0\rangle$ stands for the bosonic vacuum state, which is none other than the quantum Hall ferromagnet: i.e., $|0\rangle \equiv |QHF\rangle = \Pi_{m=0}^{N_\phi - 1} c^\dagger_{m,\uparrow}|0\rangle_F$. The equation of motion of $G(\mathbf{p}',\mathbf{p};t)$ is written as

$$\left(i\frac{\partial}{\partial t} - \omega_{\mathbf{p}}\right) G(\mathbf{p}',\mathbf{p};t) = \delta_{\mathbf{p},\mathbf{p}'}\delta(t) + \sum_{\mathbf{q}} U^e(\mathbf{q},\mathbf{p}-\mathbf{q}) g_{\mathbf{q}} G(\mathbf{p}',\mathbf{p}-\mathbf{q};t). \tag{13}$$

The zero-order approximation to the solution of Eq. (13) yields

$$G^0(\mathbf{p}',\mathbf{p};t) = \delta_{\mathbf{p},\mathbf{p}'} G^0(\mathbf{p},t), \tag{14}$$

where $G^0(\mathbf{p},t)$ stands for the bare bosonic Green's function. We now look for the expression for $G^0(\mathbf{p},t)$.

First, one needs to find the Heisenberg bosonic operator in the absence of the disorder potential. Starting with $i\partial_t b_{\mathbf{p}}(t) = [b_{\mathbf{p}}(t), \mathcal{H}_0] = \omega_{\mathbf{p}} b_{\mathbf{p}}(t)$, one then obtains $b_{\mathbf{p}}(t) = b_{\mathbf{p}} e^{-i\omega_{\mathbf{p}} t}$. Therefore, for the case $t > 0$, the free Green's function is

$$G^0(\mathbf{p},t) = -i\langle 0|b_{\mathbf{p}}(t) b^\dagger_{\mathbf{p}}|0\rangle = -ie^{-i\omega_{\mathbf{p}} t}\langle 0|b_{\mathbf{p}} b^\dagger_{\mathbf{p}}|0\rangle = -ie^{-i\omega_{\mathbf{p}} t},$$

whereas for $t < 0$, it turns out to be

$$G^0(\mathbf{p},t) = -i\langle 0|b_{\mathbf{p}}(t) b^\dagger_{\mathbf{p}}|0\rangle = -ie^{-i\omega_{\mathbf{p}} t}\langle 0|b^\dagger_{\mathbf{p}} b_{\mathbf{p}}|0\rangle = 0.$$

This solution is indeed identical to the electronic one.

Now, the cynosure is on the generic solution of the differential Eq. (13). By coupling the latter with Eq. (14) yields the integral equation

$$G(\mathbf{p}',\mathbf{p};t) = \delta_{\mathbf{p},\mathbf{p}'} G^0(\mathbf{p},t) + \int_{-\infty}^{\infty} dt' G^0(\mathbf{p},t-t') \times \sum_{\mathbf{q}} U^e(\mathbf{q},\mathbf{p}-\mathbf{q}) g_{\mathbf{q}} G(\mathbf{p}',\mathbf{p}-\mathbf{q};t). \tag{15}$$

By Fourier transforming the time in Eq. (15) to frequency and shifting $\mathbf{q} \to \mathbf{p}-\mathbf{q}$, one finds

$$G(\mathbf{p}',\mathbf{p};\omega) = \delta_{\mathbf{p},\mathbf{p}'}G^0(\mathbf{p},\omega) + G^0(\mathbf{p},\omega) \times \sum_{\mathbf{q}} U^e(\mathbf{p}-\mathbf{q},\mathbf{q}) g_{\mathbf{p}-\mathbf{q}} G(\mathbf{p}',\mathbf{q};\omega). \quad (16)$$

Here, the bare Green's function reads

$$G_0(\mathbf{p},\omega) = \frac{1}{\omega - \omega_{\mathbf{p}} + i\eta}, \quad (17)$$

where $\eta \to 0^+$ and $\omega_{\mathbf{p}}$ is given by Eq. (2). In the same way as for fermions, the solution of Eq. (16) is obtained by iteration. One gets the so-called *Born series*

$$G(\mathbf{p}',\mathbf{p}) = \sum_{n=0}^{\infty} G^{(n)}(\mathbf{p}',\mathbf{p}), \quad (18)$$

where $G^0(\mathbf{p}',\mathbf{p}) = \delta_{\mathbf{p},\mathbf{p}'}G^0(\mathbf{p})$ and for $n \geq 1$,

$$G^{(n)}(\mathbf{p}',\mathbf{p}) = G^0(\mathbf{p}) \sum_{\mathbf{q}} U^e(\mathbf{p}-\mathbf{q},\mathbf{q}) g_{\mathbf{p}-\mathbf{q}} G^{(n-1)}(\mathbf{p}',\mathbf{q}).$$

Expansion of Eq. (18) then yields

$$G(\mathbf{p}',\mathbf{p}) = \delta_{\mathbf{p},\mathbf{p}'}G^0(\mathbf{p}') + G^0(\mathbf{p}')U^e(\mathbf{p}-\mathbf{p}',\mathbf{p}')g_{\mathbf{p}-\mathbf{p}'}G^0(\mathbf{p}) + \sum_{\mathbf{q}} G^0(\mathbf{p}')U^e(\mathbf{q}-\mathbf{p}',\mathbf{p}')g_{\mathbf{q}-\mathbf{p}'}G^0(\mathbf{q})U^e(\mathbf{p}-\mathbf{q},\mathbf{q})g_{\mathbf{p}-\mathbf{q}}G^0(\mathbf{p})$$
$$+ \sum_{\mathbf{q},\mathbf{q}'} G^0(\mathbf{p}')U^e(\mathbf{q}-\mathbf{p}',\mathbf{p}')g_{\mathbf{q}-\mathbf{p}'}G^0(\mathbf{q})U^e(\mathbf{q}'-\mathbf{q},\mathbf{q})g_{\mathbf{q}'-\mathbf{q}}G^0(\mathbf{q}')U^e(\mathbf{p}-\mathbf{q}',\mathbf{q}')g_{\mathbf{p}-\mathbf{q}'}G^0(\mathbf{p}) + \cdots.$$

Due to disorder self-averaging in the limit of very large number of impurities $N_{\text{imp}} \to \infty$, with constant density n_{imp}=const., the full bosonic one-particle Green's function approaches its average value

$$\langle (G(\mathbf{p}',\mathbf{p}) - \langle G(\mathbf{p}',\mathbf{p})\rangle_{\text{imp}})^2 \rangle_{\text{imp}} \to 0, \quad (19)$$

which is

$$\langle G(\mathbf{p}',\mathbf{p})\rangle_{\text{imp}} = \delta_{\mathbf{p},\mathbf{p}'}G^0(\mathbf{p}') + \langle g_{\mathbf{p}-\mathbf{p}'}\rangle_{\text{imp}} G^0(\mathbf{p}')U^e(\mathbf{p}-\mathbf{p}',\mathbf{p}')G^0(\mathbf{p})$$
$$+ \sum_{\mathbf{q}} \langle g_{\mathbf{q}-\mathbf{p}'}g_{\mathbf{p}-\mathbf{q}}\rangle_{\text{imp}} G^0(\mathbf{p}')U^e(\mathbf{q}-\mathbf{p}',\mathbf{p}')G^0(\mathbf{q})U^e(\mathbf{p}-\mathbf{q},\mathbf{q})G^0(\mathbf{p})$$
$$+ \sum_{\mathbf{q},\mathbf{q}'} \langle g_{\mathbf{q}-\mathbf{p}'}g_{\mathbf{q}'-\mathbf{q}}g_{\mathbf{p}-\mathbf{q}'}\rangle_{\text{imp}} G^0(\mathbf{p}')U^e(\mathbf{q}-\mathbf{p}',\mathbf{p}')G^0(\mathbf{q})U^e(\mathbf{q}'-\mathbf{q},\mathbf{q})G^0(\mathbf{q}')U^e(\mathbf{p}-\mathbf{q}',\mathbf{q}')G^0(\mathbf{p}) + \cdots.$$

In the thermodynamic limit $A \to \infty$

$$\langle g_{\mathbf{q}}\rangle_{\text{imp}} = N_{\text{imp}}\delta_{\mathbf{q},0},$$

$$\langle g_{\mathbf{q}}g_{\mathbf{p}}\rangle_{\text{imp}} = N_{\text{imp}}^2\delta_{\mathbf{p},0}\delta_{\mathbf{q},0} + N_{\text{imp}}\delta_{\mathbf{q}+\mathbf{p},0},$$

$$\langle g_{\mathbf{q}'}g_{\mathbf{q}}g_{\mathbf{p}}\rangle_{\text{imp}} = N_{\text{imp}}^3\delta_{\mathbf{q}',0}\delta_{\mathbf{q},0}\delta_{\mathbf{p},0} + N_{\text{imp}}^2(\delta_{\mathbf{p}+\mathbf{q},0}\delta_{\mathbf{q}',0} + \delta_{\mathbf{q}+\mathbf{q}',0}\delta_{\mathbf{p},0} + \delta_{\mathbf{p}+\mathbf{q}',0}\delta_{\mathbf{q},0}) + N_{\text{imp}}\delta_{\mathbf{q}'+\mathbf{q}+\mathbf{p},0}. \quad (20)$$

Moreover, one has

$$U^e(0,\mathbf{p}) = U(0)f(0,\mathbf{p}) = U(0)2ie^{-|\ell(0)|^2/4}\sin\left(\frac{0\wedge\mathbf{p}}{2}\right) = 0. \quad (21)$$

Substituting Eqs. (20) and (21) into the expression for $\langle G(\mathbf{p})\rangle_{\text{imp}}$ shows that the translational invariance is recovered after the averaging $\langle G(\mathbf{p}',\mathbf{p})\rangle_{\text{imp}} = \langle G(\mathbf{p})\rangle_{\text{imp}}\delta_{\mathbf{p}',\mathbf{p}}$, where

$$\langle G(\mathbf{p})\rangle_{\text{imp}} = G^0(\mathbf{p}) + N_{\text{imp}}\sum_{\mathbf{q}} G^0(\mathbf{p})U^e(\mathbf{q}-\mathbf{p},\mathbf{p}) \times G^0(\mathbf{q})U^e(\mathbf{p}-\mathbf{q},\mathbf{q})G^0(\mathbf{p}) + N_{\text{imp}}\sum_{\mathbf{q},\mathbf{q}'} G^0(\mathbf{p})U^e(\mathbf{q}-\mathbf{p},\mathbf{p})G^0(\mathbf{q}) \times U^e(\mathbf{q}'-\mathbf{q},\mathbf{q})G^0(\mathbf{q}')U^e(\mathbf{p}-\mathbf{q}',\mathbf{q}')G^0(\mathbf{p}) + \cdots. \quad (22)$$

Therefore, there is no first-order Born scattering contribution to the bosonic self-energy. Moreover, it is possible to show that all odd order contributions to the self-energy vanish (see Appendix A).

This result is expressed diagrammatically in Fig. 1. It was shown[22] that the disorder averaged Green's function can also be expressed as

$$\langle G(\mathbf{p})\rangle_{\text{imp}} = \frac{1}{\omega - \omega_{\mathbf{p}} - \Sigma(\mathbf{p},\omega)}. \quad (23)$$

Hence, the self-energy must now be computed. The low-density weak-scattering approximation will be used throughout the calculations. Low density means that the number of

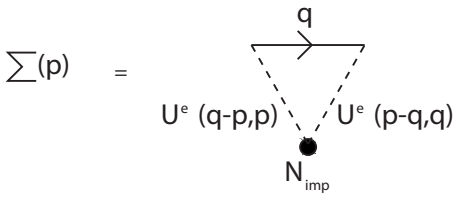

FIG. 2. Self-energy in the low-density weak-scattering approximation.

disorder atoms present in the system is taken to be much lower than the number of electrons and allows one to keep only the self-energy diagrams with a single impurity and to neglect diagrams with crossed impurity lines. On the other hand, for weak impurity potential U one can neglect diagrams with multiple scattering from one impurity, keeping only the first and the second Born scatterings from a given atom.[22] The problem then reduces to solving the diagrammatic expression shown in Fig. 2.

The self-energy can be evaluated in two different manners: (1) the bare approximation that uses the bare propagator G^0 and (2) the self-consistent approximation that uses the full disorder self-averaged Green's function $\langle G\rangle_{\text{imp}}$. Therefore, for generality we will use the propagator $G(\mathbf{q},\omega)$, which is going to be specified further for each particular case. This yields algebraically

$$\Sigma(\mathbf{p},\omega) = N_{\text{imp}}\sum_{\mathbf{q}} U^e(\mathbf{q}-\mathbf{p},\mathbf{p})G(\mathbf{q},\omega)U^e(\mathbf{p}-\mathbf{q},\mathbf{q})$$
$$= N_{\text{imp}}\sum_{\mathbf{q}} U(\mathbf{q}-\mathbf{p})f(\mathbf{q}-\mathbf{p},\mathbf{p})G(\mathbf{q},\omega)U(\mathbf{p}-\mathbf{q})f(\mathbf{p}-\mathbf{q},\mathbf{q}), \tag{24}$$

where Eq. (10) was substituted in the second line.

In this work, the impurity potential is assumed to be short range, i.e., $U(\mathbf{q})$=constant. An uniform potential in momentum space is attained from a delta function interaction in real space, $U(\mathbf{r})=U\delta(\mathbf{r})$ [such that $U(\mathbf{q})=(1/A)\int d\mathbf{r}e^{i\mathbf{q}\cdot\mathbf{r}}U\delta(\mathbf{r})=U/A$]. Thus, this model assumes that the bosons (and therefore the electrons) collide directly with the impurity "atoms" that constitute the effective disorder potential; in reality, most of the impurities are located away from the 2DEG. Thus, one has

$$\Sigma(\mathbf{p},\omega) = N_{\text{imp}}\sum_{\mathbf{q}}\left(\frac{U}{A}\right)^2\left[2ie^{-|\ell(\mathbf{q}-\mathbf{p})|^2/4}\sin\left(\frac{(\mathbf{q}-\mathbf{p})\wedge\mathbf{p}}{2}\right)\right]$$
$$\times G(\mathbf{q},\omega)\left[2ie^{-|\ell(\mathbf{p}-\mathbf{q})|^2/4}\sin\left(\frac{(\mathbf{p}-\mathbf{q})\wedge\mathbf{q}}{2}\right)\right]$$
$$= 4N_{\text{imp}}\left(\frac{U}{A}\right)^2\sum_{\mathbf{q}} e^{-|\ell(\mathbf{q}-\mathbf{p})|^2/2}\sin^2\left(\frac{\mathbf{q}\wedge\mathbf{p}}{2}\right)G(\mathbf{q},\omega). \tag{25}$$

One then expands the argument of the exponential

$$e^{-|\ell(\mathbf{q}-\mathbf{p})|^2/2} = e^{-|\ell\mathbf{q}|^2/2}e^{-|\ell\mathbf{p}|^2/2}e^{\ell^2\mathbf{q}\cdot\mathbf{p}} = e^{-(\ell q)^2/2}e^{-(\ell p)^2/2}e^{\ell^2 qp\cos\phi}. \tag{26}$$

Here, ϕ denotes the angle between vectors $\mathbf{q}$ and $\mathbf{p}$. Furthermore, the summation is transmuted into an integration through the use of the formula,

$$\sum_{\mathbf{q}} = \frac{A}{4\pi^2}\int d^2q = \frac{A}{4\pi^2}\int_0^\infty dqq\int_0^{2\pi} d\theta. \tag{27}$$

The angle θ is taken arbitrarily on the plane containing the vector $\mathbf{q}$, therefore, one is free to set $\theta=\phi$. The sine squared term in Eq. (25) can be rewritten as $\sin^2(\mathbf{q}\wedge\mathbf{p}/2)=[1-\cos(\mathbf{q}\wedge\mathbf{p})]/2=[1-\cos(\ell^2 qp\sin\phi)]/2$. We also assume rotation invariance of the Green's function $G(\mathbf{q},\omega)=G(q,\omega)$. Hence, the self-energy is also rotation invariant and can be expressed as

$$\Sigma(p,\omega) = 4n_{\text{imp}}U^2\int_0^\infty\frac{dq}{2\pi}qe^{-(\ell q)^2/2}e^{-(\ell p)^2/2}G(q,\omega)$$
$$\times\int_0^{2\pi}\frac{d\phi}{2\pi}e^{\ell^2 qp\cos\phi}\frac{1}{2}[1-\cos(\ell^2 qp\sin\phi)], \tag{28}$$

where $n_{\text{imp}}=N_{\text{imp}}/A$ stands for the impurity density. After a straightforward calculation (see Appendix B), we find

$$\Sigma(p,\omega) = 4n_{\text{imp}}U^2\int_0^\infty\frac{dq}{2\pi}qe^{-(\ell q)^2/2}e^{-(\ell p)^2/2}G(q,\omega)$$
$$\times\frac{1}{2}[I_0(\ell^2 qp)-1]. \tag{29}$$

Rescaling the momenta by $\mathbf{q},\mathbf{p}\to\mathbf{q}/\ell,\mathbf{p}/\ell$ simplifies the self-energy to

$$\Sigma(p,\omega) = \frac{u}{4}\epsilon_B^2 e^{-p^2/2}\int_0^\infty dqqe^{-q^2/2}[I_0(qp)-1]G(q,\omega), \tag{30}$$

where the various prefactors, including the disorder potential strength and the impurity density, can be regrouped into a single convenient parameter

$$u = \frac{4n_{\text{imp}}U^2}{\pi\ell^2\epsilon_B^2}, \tag{31}$$

which will be dubbed the *disorder strength*. Thus, u is a dimensionless parameter that measures the disorder interaction strength relative to the Coulomb interaction, $u\approx(E_{\text{dis}}/E_{\text{coul}})^2$. The above self-energy expression will be evaluated in two different ways: (i) first-order corrections in u and (ii) self-consistently.

Bare approximation

In the previous section we have shown that to the lowest order in $\epsilon_B/\hbar\omega_c$ and in the disorder strength u, the electron-electron interactions and disorder are taken into account by

the magnon self-energy in the bare approximation, i.e., for $u \ll 1$ the self-energy Eq. (30) becomes

$$\Sigma(p,\omega) = \frac{u}{4}\epsilon_B^2 e^{-p^2/2}\int_0^\infty dqqe^{-q^2/2}[I_0(qp)-1]G^0(q,\omega). \tag{32}$$

After substituting Eq. (17) into the above, we obtain

$$\Sigma(p,\omega) = \frac{u}{4}\epsilon_B^2 e^{-p^2/2}\int_0^\infty dqqe^{-q^2/2}\frac{I_0(qp)-1}{\omega-\omega_{\mathbf{q}}+i\eta}. \tag{33}$$

We find then the real and imaginary parts of the self-energy

$$\mathrm{Re}\,\Sigma(p,\omega) = \frac{u}{4}\epsilon_B^2 e^{-p^2/2}\mathcal{P}\int_0^\infty dqqe^{-q^2/2}\frac{I_0(qp)-1}{\omega-\omega_q}, \tag{34}$$

$$\mathrm{Im}\,\Sigma(p,\omega) = -\frac{u}{4}\epsilon_B^2 e^{-p^2/2}\int_0^\infty dqqe^{-q^2/2} \times[I_0(qp)-1]\pi\delta(\omega-\omega_q). \tag{35}$$

The above equations can be evaluated analytically in the long wavelength approximation, which is done in Appendix C. Here, one uses the complete bosonic dispersion relation given by Eq. (2). As a result, one can only solve the imaginary self-energy numerically; that task is not performed here. We concentrate, instead, on the real part.

The renormalized energy of the bosons (including the disorder contribution) is obtained by looking at the poles of the full disorder self-averaged Green's function in Eq. (23), $\omega - \omega_{\mathbf{p}} - \mathrm{Re}\,\Sigma(\mathbf{p},\omega)=0$, such that the renormalized dispersion relation is determined from Eq. (34)

$$\omega = g + \epsilon_B\left[1 - e^{-p^2/4}I_0\left(\frac{p^2}{4}\right)\right] + \frac{u}{4}\epsilon_B^2 e^{-p^2/2}\mathcal{P}\int_0^\infty dqqe^{-q^2/2} \times \frac{I_0(qp)-1}{\omega - \left\{g + \epsilon_B\left[1 - e^{-q^2/4}I_0\left(\frac{q^2}{4}\right)\right]\right\}}. \tag{36}$$

The corresponding plot is illustrated on Fig. 3(a). One can notice that at not too large momenta (i.e., near $|p\ell|=1$) there exists already a substantial difference between the bare (long wavelength) and bare (full k) approximations.

Now, the renormalized spin stiffness is sought for. For the sake of convenience, one begins by introducing the variables $\tilde{\omega}$, $\tilde{g}=\omega/\epsilon_B$, g/ϵ_B and rewriting Eq. (36) as

$$\tilde{\omega} - \tilde{g} = 1 - e^{-p^2/4}I_0\left(\frac{p^2}{4}\right) + \frac{u}{4}e^{-p^2/2}\mathcal{P}\int_0^\infty dqqe^{-q^2/2}\frac{I_0(qp)-1}{(\tilde{\omega}-\tilde{g}) - \left[1 - e^{-q^2/4}I_0\left(\frac{q^2}{4}\right)\right]}. \tag{37}$$

One then expands the above in powers of p, and takes only the p^2 terms,

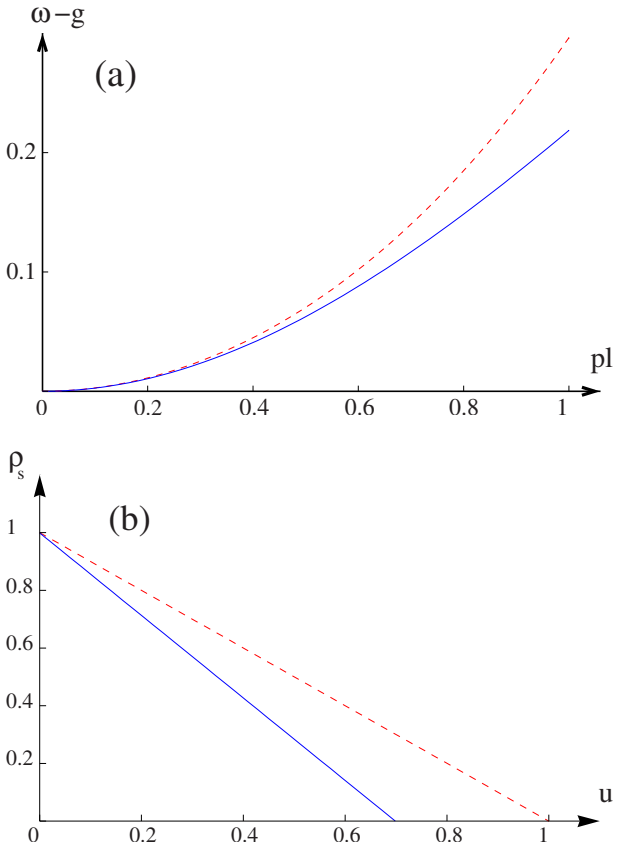

FIG. 3. (Color online) (a) Renormalized dispersion in the bare full k approximation (blue/solid gray), in units of the Coulomb energy $e^2/(\epsilon\ell)$, contrasted with the one in the bare long-wavelength approximation (red/dashed gray), both as functions of the momentum $|p\ell|$ and at $u=0.1$. (b) Renormalized spin stiffness in the bare full k approximation (blue/solid gray) and in the bare long-wavelength approximation (red/dashed gray). Notice that using the bare Green's function G_0 we find a transition from a ferromagnetic to a paramagnetic phase, whereas using G in the self-consistent approximation we find a transition into a spin-glass phase (see next section).

$$\tilde{\omega} - \tilde{g} = \frac{p^2}{4} - \frac{u}{4}\frac{p^2}{4}\int_0^\infty dq\frac{q^3e^{-q^2/2}}{\left[1 - e^{-q^2/4}I_0\left(\frac{q^2}{4}\right)\right]} + \cdots = \frac{p^2}{4}\left[1 - \frac{u}{4}(5.72)\right] + \cdots. \tag{38}$$

The renormalized spin stiffness then reads

$$\rho_s = \frac{\epsilon_B}{4}(1 - 1.43u). \tag{39}$$

Equation (39) is the main result of this section and agrees with the results previously obtained by Doretto.[23] The above expression was derived in the bare approximation, which takes into account only the lowest order corrections in u. Such assumption is only true in the realm of weak-disorder scattering $u \ll 1$.[24] It can be seen that the renormalized spin stiffness decreases linearly in this approximation. A naive

extrapolation of this dependence to the region of finite and strong disorder strength $u \sim 1$ shows that there is a certain value $u_p = 0.7$, for which the renormalized spin stiffness vanishes (in the long wavelength approximation $u_p = 1$) and which is outside the range of validity of the bare approximation, see Fig. 3(b). Green[1] explains that a vanishing renormalized spin stiffness at a threshold disorder strength means that the 2DEG at $\nu = 1$ undergoes a quantum phase transition from a ferromagnetic state to a paramagnetic one. Thus, one can infer that the quantum Hall ferromagnet undergoes a disorder-driven quantum phase transition to a paramagnetic state at critical disorder strength $u_p = 0.7$. It is also interesting to remark that Green established this general finding in the domain of the weak-disorder limit (though in the context of a different model). The results obtained in this section cannot be directly compared quantitatively with those of Green,[1] Sinova *et al.*,[2] and Rapsch *et al.*[3] In addition to the fact that the model used in the studies of Green is different, he does not complement his proposition on the vanishing of the renormalized spin stiffness with some quantitative results. Sinova *et al.*[2] used a disparate variable in the ratio of the interaction strength to the Landau-level-broadening disorder energy scale. Finally, Rapsch *et al.*[3] performed their numerical calculations on a semiclassical spin model.

In the next section, we evaluate the self-energy using the so-called self-consistent approximation, which is more appropriate for $u \sim 1$, and show that the renormalized spin stiffness drastically changes its behavior, leading to completely different conclusions about the phase transition.

IV. SELF-CONSISTENT APPROXIMATION

In Ref. 25 it was demonstrated that summing the most relevant diagrams, which are "paired" and without "intersections," results into the self-consistent approximation, which can be applied even for $u \sim 1$. The self-consistent approximation means that the self-energy is evaluated with the total disorder averaged Green's function in Eq. (23) instead of the bare one. Evidently, for $u \ll 1$ the self-consistent and the bare approximations become equivalent. However, for the case of strong impurity potential U the contribution from the other diagrams, not included in the self-consistent approximation, may become non-negligible and the approximation may fail to grasp some essential features. In what follows we assume that this is not the case and, therefore, one has [see Eq. (30)]

$$\Sigma_u(p,\omega) = \frac{u}{4}\epsilon_B^2 e^{-p^2/2}\int_0^\infty dqqe^{-q^2/2}[I_0(qp)-1]\langle G_u(q,\omega)\rangle_{\text{imp}}. \tag{40}$$

Now, by referring to the computations carried out in the previous section and substituting Eq. (23), one gets

$$\Sigma_u(p,\omega) = \frac{u}{4}\epsilon_B^2 e^{-p^2/2}\int_0^\infty dqqe^{-q^2/2}\frac{I_0(qp)-1}{\omega-\omega_q-\Sigma_u(q,\omega)}. \tag{41}$$

Using that

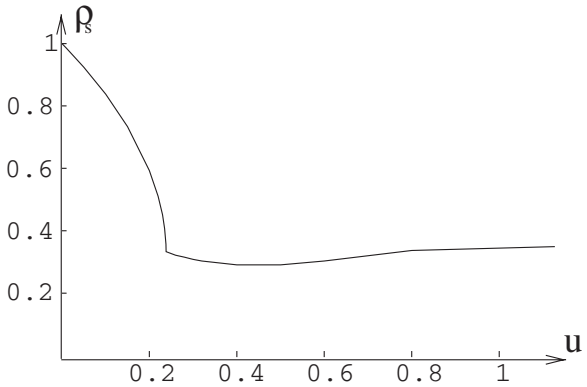

FIG. 4. Real part of the renormalized spin stiffness as a function of the disorder strength u in units of $\epsilon_B/4$.

$$I_0(qp) - 1 = \sum_{n=1}^{\infty}\frac{(qp)^{2n}}{(2^n n!)^2}, \tag{42}$$

one has

$$\Sigma_u(p,\omega) = \frac{u}{4}\epsilon_B^2 e^{-p^2/2}\sum_{n=1}^{\infty}\frac{p^{2n}}{(2^n n!)^2}\int_0^\infty dq\frac{q^{2n+1}e^{-q^2/2}}{\omega-\omega_q-\Sigma_u(q,\omega)}. \tag{43}$$

Thus, one can write

$$\Sigma_u(p,\omega) = e^{-p^2/2}\sum_{n=1}^{\infty}\sigma_n(\omega,u)p^{2n} \tag{44}$$

with

$$\sigma_n(\omega,u) = \frac{u}{4(2^n n!)^2}\epsilon_B^2\int_0^\infty dq\frac{q^{2n+1}e^{-q^2/2}}{\omega-\omega_q-\Sigma_u(q,\omega)}. \tag{45}$$

Using such expansion allows one to promptly get a numerical solution by iterations (see Fig. 4). The convergence of the iterative solution is rather good up to some value of the disorder concentration u_c. However, when $u \to u_c$, we find that $\partial_u\sigma_1(0,u) \to \infty$. Therefore, it would be desirable to derive an analytical solution in the neighborhood of u_c. For convenience, we omit the arguments of σ_n in our notation in the next part. In general,

$$\frac{\partial\Sigma_u(p,\omega)}{\partial u} = \frac{\Sigma_u(p,\omega)}{u} + \frac{u}{4}\epsilon_B^2 e^{-p^2/2}\int_0^\infty dqqe^{-q^2/2} \times\frac{I_0(qp)-1}{[\omega-\omega_q-\Sigma_u(q,\omega)]^2}\frac{\partial\Sigma_u(q,\omega)}{\partial u}, \tag{46}$$

or equivalently

$$\frac{\partial\sigma_n}{\partial u} = \frac{\sigma_n}{u} + \frac{u}{4(2^n n!)^2}\epsilon_B^2\int_0^\infty dq\frac{q^{2n+1}e^{-q^2/2}}{[\omega-\omega_q-\Sigma_u(q,\omega)]^2}\frac{\partial\Sigma_u(q,\omega)}{\partial u}. \tag{47}$$

Introducing for simplicity

$$F_n \equiv \epsilon_B^2 \int_0^\infty dq \frac{q^{2n+1} e^{-q^2}}{[\omega - \omega_q - \Sigma_u(q,\omega)]^2} \tag{48}$$

one finds

$$\frac{\partial \sigma_n}{\partial u} = \frac{\sigma_n}{u} + \frac{u}{4(2^n n!)^2} \sum_{k=1}^{\infty} F_{n+k} \frac{\partial \sigma_k}{\partial u}. \tag{49}$$

Introducing a matrix notation

$$B_{m,n} \equiv \delta_{m,n} - \frac{u F_{m+n}}{2^{m+n+2} m\,!\, n!}, \tag{50}$$

Eq. (49) reads

$$\sum_{k=1}^{\infty} B_{n,k} 2^k k\,! \frac{\partial \sigma_k}{\partial u} = \frac{2^n n\,!\, \sigma_n}{u}. \tag{51}$$

Its solution is found by computing the inverse matrix to Eq. (50) and has the form

$$\frac{\partial \sigma_n}{\partial u} = \frac{2^{-n}}{u n!} \sum_{k=1}^{\infty} B_{n,k}^{-1} 2^k k\,!\, \sigma_k. \tag{52}$$

Substituting this result into

$$\frac{d[\det(B)^2]}{du} = 2 \det(B) \left[\frac{\partial \det(B)}{\partial u} + \sum_{n=1}^{\infty} \frac{\partial \det(B)}{\partial \sigma_n} \frac{\partial \sigma_n}{\partial u} \right],$$

yields

$$\frac{d[\det(B)^2]}{du} = -\kappa(u), \tag{53}$$

where

$$\kappa(u) \equiv -2 \det(B) \frac{\partial \det(B)}{\partial u} - 2 \det(B) \sum_{n,k=1}^{\infty} \frac{\partial \det(B)}{\partial \sigma_n} \frac{2^{k-n} k!}{u n!} \sigma_k B_{n,k}^{-1}$$

with

$$\frac{\partial \det(B)}{\partial u} = \det(B) \mathrm{Tr}\left(B^{-1} \frac{\partial B}{\partial u} \right) = -\frac{1}{u} \det(B) \mathrm{Tr}(B^{-1} - I)$$

and

$$\frac{\partial \det(B)}{\partial \sigma_n} = -\sum_{m,k=1}^{\infty} \det(B) B_{k,m}^{-1} \frac{u}{2^{m+k+2} m\,!\, k!} \frac{\partial F_{m+k}}{\partial \sigma_n},$$

where

$$\frac{\partial F_m}{\partial \sigma_n} = 2 \epsilon_B^2 \int_0^\infty dq \frac{q^{2n+2m+1} e^{-3q^2/2}}{[\omega - \omega_q - \Sigma(q,\omega)]^3}.$$

Suppose that $\det(B) \to 0$ when $u \to u_c$. In this case $B^{-1} \det(B)$ remains finite, as well as $\kappa(u)$. This suggests that

$$\frac{\partial \sigma_n}{\partial u} \to \infty, \tag{54}$$

when $u \to u_c$, since the other terms are finite. Moreover, if $\kappa(u)$ is a smooth function around u_c, such that $\kappa(u_c) \approx \kappa(u_0)$ for some u_0 from the neighborhood of u_c, then according to Eq. (53) there holds

$$\det[B(u)] = \sqrt{\kappa(u_c)(u_c - u)} + \mathcal{O}(u_c - u). \tag{55}$$

It follows then from Eq. (55) that $u_c \approx u_0 + \det[B(u_0)]^2 / \kappa(u_0)$ as long as $u_0 \to u_c$. However, the analysis of the infinite dimensional matrix B and its determinant is quite complicated, which forces us to use an approximate solution, where we keep only the first 40 terms in the expansion, thus reducing the dimension of the matrices to 40×40. In the absence of Zeeman splitting ($g=0$), for $\omega=0$, and $u_0=0.238$ one finds, setting $\epsilon_B=1$, that $\det[B(u_0)] = 0.0551776$ and $\kappa(u_0)=9.7945$, which yields $u_c=0.238311$ in excellent agreement with the numerical solution. The approximation also allows to check the validity of Eq. (52), which yields $\sigma_1' = -9.384$ at the point $u_0=0.238$ (here the prime stands for the partial derivative with respect to u). On the other hand, the numerical solution for the two points $u_0 = 0.238$ and $u_1 = 0.23801$ yields $\Delta\sigma_1 / \Delta u = -9.463$, which agrees reasonably well with the previous result. The main difference stems from the fact that $u_0=0.238$ is rather close to the critical point u_c, where the derivative diverges, so the value $\Delta u = 10^{-5}$ is still rather large and, of course, computational errors and approximation with finite number of terms make the result not very precise. Furthermore, it follows from Eq. (52) that $\sigma_n' \det(B)$ remains finite with $u \to u_c$. Thus,

$$\sigma_n(u) - \sigma_n(u_0) = \int_{u_0}^{u} dv \frac{\partial \sigma_n(v)}{\partial v} \approx \frac{\det[B(u_0)] \sigma_n'(u_0)}{\sqrt{\kappa(u_0)}} \int_{u_0}^{u} dv (u_c - v)^{-1/2}, \tag{56}$$

which leads to

$$\sigma_n(u) = \sigma_n(u_c) + [\sigma_n(u_0) - \sigma_n(u_c)] \frac{\det[B(u)]}{\det[B(u_0)]} \tag{57}$$

after performing the integration, where $\sigma_n(u_c) - \sigma_n(u_0) = 2(u_c - u_0)\sigma_n'(u_0)$. From this analytic solution one may observe that σ_n and, consequently, $\Sigma(\mathbf{p}, \omega)$ acquires an imaginary part when $u > u_c$. In particular, considering $n=1$, for the case at hand $\sigma_1(u_0) = -0.161742$ and $\sigma_1(u_c) = -0.167576$. Defining

$$\alpha \equiv -\lim_{u \to u_c} \frac{2\sigma_1'(u) \det[B(u)]}{\sqrt{\kappa(u)}}, \tag{58}$$

the value of α can be evaluated without any fitting parameters directly from Eqs. (52) and (54), which yields $\alpha = 0.331$. It follows directly from the above that the renormalized spin stiffness now obeys

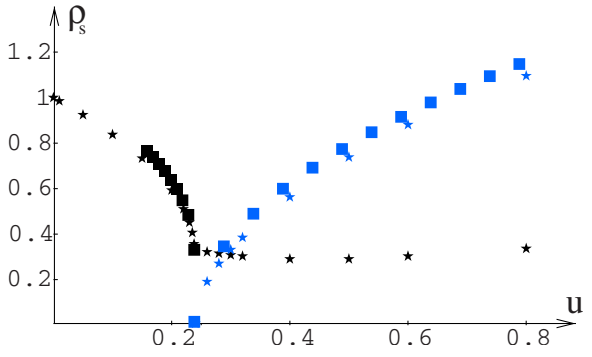

FIG. 5. (Color online) The real part of the renormalized spin stiffness in units of $\epsilon_B/4$ is shown in black as a function of the disorder strength u and the imaginary part is shown in blue (gray) color. (Square—analytic solution, star—numerical).

$$\rho_s(u) = \rho_s(u_c) + \alpha\epsilon_B\sqrt{u_c - u}, \tag{59}$$

where $\rho_s(u_c) = \epsilon_B[\sigma_1(u_c) + 1/4]$. Both numerical and analytic results for $\rho_s(u)$ are plotted in Fig. 5, which shows that the analytic solution remains in excellent agreement with the numerical one even for those values of u, which are far from the critical point u_c. The whole behavior of the renormalized spin stiffness is very similar to the one obtained by Chalker and co-workers,[3] describing a spin-glass phase transition. Moreover, such dependence of the renormalized spin stiffness as a square root function of a control parameter was already observed previously by Shender,[18] as well as by Avgin *et al.*[19] They considered the two- and three-dimensional $\pm J$ Heisenberg spin-glass models in a ferromagnetic ground state due to a strong external magnetic field. They found that for a certain value of the control parameter, $\rho_s(u)$ acquires an imaginary part. The real part of $\rho_s(u)$ is proportional to the spin-wave stiffness, whereas the imaginary part is proportional to the damping of the spin-wave excitations, thus signaling localization. It was argued that when the frequency of the spin-wave excitation ω multiplied by its lifetime τ is $\omega\tau = \mathrm{Re}[\rho_s(u)]/\mathrm{Im}[\rho_s(u)] < 1$, then the spin waves are completely localized. As we can see from the Fig. 5, the condition of localization is already satisfied for the values of the disorder strength starting from $u = 0.3$. The calculations presented in the Appendix D contain a strong indication that the Pauli susceptibility diverge at the point $u = u_c$, suggesting a phase transition from a ferromagnetic ground state to a spin-glass state,[3] since the spin waves become localized.

Our discussion was mainly concerned with the static case $\omega = 0$. However, our approach allows to find $\Sigma(p, \omega)$ for any given ω. The dispersion spectrum in the self-consistent approximation then satisfies $\omega - \omega_p - \mathrm{Re}\,\Sigma(p, \omega) = 0$.

A similar model was considered by Burmistrov[4] for the case of high Landau levels $\nu \gg 1$. There are several common points in both models. (i) In our model the disorder is characterized by a single parameter $u \sim n_{\mathrm{imp}}U^2$ (instead of the two independent n_{imp} and U), which scales linearly in n_{imp} and quadratically in U. In Ref. 4, the disorder parameter τ^{-1} scales exactly in the same way. Thus, the disorder is characterized by essentially the same single parameter in both models, i.e., the case of weak density and moderate impurity potential is considered equivalent to the case of moderate density and weak impurity potential. In our work this is a consequence of the self-consistent approximation, while in the work[4] this is a feature of the model itself, relying on the Gaussian distribution. Going beyond the self-consistent approximation and including the other type of diagrams will introduce more (higher order in U) parameters depending on n_{imp} and U, for example, $n_{\mathrm{imp}}U^4$. On the other hand, the introduction of another parameter in Ref. 4, which scales like $n_{\mathrm{imp}}U^4$, would require to include higher orders of the impurity potential in the distribution function, which makes it essentially non-Gaussian. (ii) The interactions are taken into account basically at the same level of approximation: quadratic in the bosonic field when integrating out lower Landau levels in Ref. 4 and RPA in a broad sense (including the ladder diagrams) in our work. (iii) The calculations in both works predict finite lifetime of the quasiparticle excitations due to the disorder scattering.

The most crucial difference in the predicted results is that the spin stiffness increases with the increase in the strength of disorder in Ref. 4 ($\nu \gg 1$) and decreases in our model ($\nu = 1$). The difference does not stem from the different computational approaches but is fully attributed to the difference in the filling factor ν considered in the two models. In the case $\nu \gg 1$, the disorder suppresses the effect of screening from the lower Landau levels, thus resulting into an increase in the electron-electron interactions, which "strengthens" the ferromagnetic state and leads to an increase in the spin stiffness. On the other hand, for $\nu = 1$, there is no screening from the lower lying Landau levels, since all the electrons are already in the lowest one, and the presence of disorder leads only to a "weakening" of the ferromagnetic order and thus decreases the spin stiffness, as was shown by a number of authors.[1–3]

V. CONCLUSIONS AND OUTLOOK

This paper accounts for the presence of both disorder and interactions in a 2DEG at Landau-level filling factor $\nu = 1$, whose ground state constitutes the well-known quantum Hall ferromagnet. The bosonization technique developed by Doretto *et al.*[12] was employed in order to facilitate the treatment of both disorder and interactions in this strongly correlated system. The bosonization procedure consists in treating the spin-wave (magnon) excitation as a boson such that the fermionic Hamiltonian of the system can be approximately recast into a Hamiltonian expressed in terms of bosonic operators. As a consequence, the interaction between electrons up to RPA level was incorporated within the bare propagator that represents the free boson. The intent was then to identify a disorder-driven quantum phase transition to a nonferromagnetic state by analyzing the behavior of the renormalized spin stiffness as a function of the disorder strength, which itself corresponds to the ratio squared of the disorder energy scale to the Coulomb energy one. To achieve this aim, first, we derived the bosonic expression for the Hamiltonian of the system. In the second stage, the focus was on seeking out the disorder self-averaged Green's function, which is the full bosonic Green's function averaged over the impurity positions. Then, by using the Dyson's equation, we obtained a

diagrammatic representation of the self-energy. The latter was subsequently computed within the framework of the low-density weak-scattering approximation. Low density means that the number of disorder atoms present in the system is taken to be much lower than the number of electrons, while the weak-scattering approximation signifies that the scattering potential induced by a given impurity atom is weak, such that only the first- and second-order Born scatterings are accounted for. As a result, the self-energy corresponded to a single diagram. Furthermore, the self-energy was evaluated in three different approximations: (1) the bare (long wavelength) approximation, which consists in using the bare bosonic propagator and keeping the lowest order terms in momenta, (2) the bare (full k) approximation, which uses as well the bare bosonic propagator but with all the momenta terms kept in the calculation, and, finally, (3) the self-consistent approximation, which uses the full disorder averaged Green's function instead of the bare one in the self-energy diagram. Then, the renormalized spin stiffness was determined by extracting the coefficient of the quadratic term in the dispersion relation together with the contribution from the self-energy. In the case of the bare (long-wavelength) approximation, the spin stiffness was found to vanish linearly at the disorder strength $u_p=1$. For the bare (full k) scheme, the spin stiffness also vanished linearly, but at the disorder strength $u_p=0.7$. These results suggest the occurrence of a disorder-driven quantum phase transition from the ferromagnetic phase to a paramagnetic one at the critical value $u_p=0.7$. However, the critical values are clearly outside the range of validity of the bare approximation, which is applicable for $u \ll 1$. Lastly, the self-consistent calculation, which is more applicable for $u \sim 1$, revealed a completely different behavior: the real part of the renormalized spin stiffness also initially decreases with increasing the disorder strength u, coinciding in the region $u \ll 1$ with the one obtained in the bare approximation, but then it saturates without reaching zero beyond a critical value u_c, at which it (and the self-energy) acquires an imaginary component. According to the Shender criterium,[18] the spin waves become completely localized when the imaginary part of the renormalized spin stiffness becomes larger than the real part, which occurs in our system for $u > 0.3$ (see Fig. 5).

The physical mechanism behind a phase transition from the ferromagnetic ground state can be understood by considering electrons completely filling the lowest Landau level ($\nu=1$) in the presence of some inhomogeneous electrostatic background (disorder). Then, for sufficiently strong impurity potential, by adjusting the electron density to the electrostatic background, the system would gain more energy than is needed to rearrange the spin configuration. In this case the ferromagnetic state does not minimize the total energy of the system and a phase transition should take place. This quantum phase transition could be detected by calculating the behavior of the magnetic susceptibility as a function of the disorder strength. A sharp peak is anticipated at the transition point. In particular, if the energy cost for exciting a spin wave is less than the gain in the electrostatic energy, then the renormalized spin stiffness becomes negative and the system undergoes a phase transition to a paramagnetic state with zero local magnetization. On the other hand, as it was argued by Rapsch *et al.*,[3] in the case of a smoothly varying impurity potential, keeping nonzero local magnetization is still energetically favorable and the electrostatic energy is lowered by screening the impurity potential due to the formation of spin textures. At strong disorder such phase would correspond to a spin glass and the spin textures might be considered as the localized spin waves. Thus, the character of the phase transition might depend on the nature of the disorder. The calculations performed within our model indicate that the Pauli susceptibility diverges at the same critical point of the disorder strength u_c, where an imaginary part of the renormalized spin stiffness appears, thus suggesting a phase transition to a spin-glass phase.

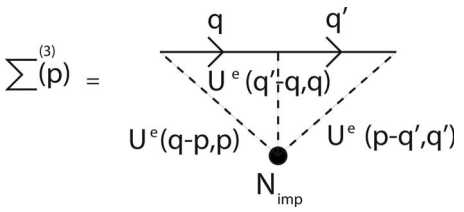

FIG. 6. Diagrammatic representation of the third-order diagrammatic contribution to the self-energy.

Our approach can be extended for the case of bilayer systems in the presence of disorder. In fact, Fertig and Murthy[26] have already considered such systems. Thus, it would be interesting to apply our formalism to the case of a bilayer system with the total filling factor $\nu_T=1$ and compare the results.

ACKNOWLEDGMENTS

We acknowledge insightful discussions with T. Giamarchi, A. Lazarides, and L. Cugliandolo. We also would like to thank R. L. Doretto for proposing us this interesting problem. This work was partially supported by the Netherlands Organization for Scientific Research (NWO).

APPENDIX A: THIRD-ORDER DIAGRAM

Let us now evaluate the third-order diagram contribution to the self-energy. Its diagrammatic representation is shown in Fig. 6. Algebraically, we have

$$\begin{aligned}\Sigma^{(3)}(\mathbf{p},\omega) &= N_{\mathrm{imp}} \sum_{\mathbf{q},\mathbf{q}'} U^e(\mathbf{q}-\mathbf{p},\mathbf{p}) G(\mathbf{q},\omega) \\ &\quad \times U^e(\mathbf{q}'-\mathbf{q},\mathbf{q}) G(\mathbf{q}',\omega) U^e(\mathbf{p}-\mathbf{q}',\mathbf{q}') \\ &= N_{\mathrm{imp}} \sum_{\mathbf{q},\mathbf{q}'} U(\mathbf{q}-\mathbf{p}) f(\mathbf{q}-\mathbf{p},\mathbf{p}) G(\mathbf{q},\omega) \\ &\quad \times U(\mathbf{q}'-\mathbf{q}) f(\mathbf{q}'-\mathbf{q},\mathbf{q}) \\ &\quad \times G(\mathbf{q}',\omega) U(\mathbf{p}-\mathbf{q}') f(\mathbf{p}-\mathbf{q}',\mathbf{q}'). \end{aligned} \tag{A1}$$

Here again, the impurity potential is short range $U(\mathbf{q})$ = constant = U/A. By replacing all the functions defined previously, we find

$$\Sigma^{(3)}(\mathbf{p},\omega) = N_{\text{imp}} \sum_{\mathbf{q},\mathbf{q}'} \left(\frac{U}{A}\right)^3 \left[2ie^{-|\ell(\mathbf{q}-\mathbf{p})|^2/4} \sin\left(\frac{(\mathbf{q}-\mathbf{p})\wedge\mathbf{p}}{2}\right)\right] G(\mathbf{q},\omega)$$
$$\times \left[2ie^{-|\ell(\mathbf{q}'-\mathbf{q})|^2/4} \sin\left(\frac{(\mathbf{q}'-\mathbf{q})\wedge\mathbf{q}}{2}\right)\right] G(\mathbf{q}',\omega) \left[2ie^{-|\ell(\mathbf{p}-\mathbf{q}')|^2/4} \sin\left(\frac{(\mathbf{p}-\mathbf{q}')\wedge\mathbf{q}'}{2}\right)\right]$$
$$= N_{\text{imp}} \sum_{\mathbf{q},\mathbf{q}'} \left(\frac{U}{A}\right)^3 (2i)^3 \underbrace{e^{-|\ell(\mathbf{q}-\mathbf{p})|^2/4} e^{-|\ell(\mathbf{p}-\mathbf{q}')|^2/4} e^{-|\ell(\mathbf{q}'-\mathbf{q})|^2/4}}_{\text{Term a}} \underbrace{\sin\left(\frac{\mathbf{q}\wedge\mathbf{p}}{2}\right)\sin\left(\frac{\mathbf{p}\wedge\mathbf{q}'}{2}\right)}_{\text{Term b}}$$
$$\times \underbrace{\sin\left(\frac{\mathbf{q}'\wedge\mathbf{q}}{2}\right)}_{\text{Term c}} G(\mathbf{q},\omega) G(\mathbf{q}',\omega). \tag{A2}$$

It is clear that Terms a and b are symmetric under the interchange $\mathbf{q}\leftrightarrow\mathbf{q}'$ while Term c is antisymmetric. Thus, one has

$$\Sigma^{(3)}(\mathbf{p},\omega) = 0. \tag{A3}$$

This result holds true in both the full bare and self-consistent approximations.

As a matter of fact, due to the antisymmetric property of the wedge product within the sine term, it turns out that all odd order terms vanish.

APPENDIX B: DETAILED DERIVATION OF THE SELF-ENERGY

We prove here the expressions (34) and (35). We begin with the expression of the self-energy given by Eq. (28)

$$\Sigma(p,\omega) = 4n_{\text{imp}}U^2 \int_0^\infty \frac{dq}{2\pi} q e^{-(\ell q)^2/2} e^{-(\ell p)^2/2} G(q,\omega)$$
$$\times \int_0^{2\pi} \frac{d\phi}{2\pi} e^{\ell^2 qp\cos\phi} \frac{1}{2}[1-\cos(\ell^2 qp\sin\phi)]. \tag{B1}$$

One first deals with the polar integral,

$$\int_0^{2\pi} \frac{d\phi}{2\pi} e^{\ell^2 qp\cos\phi} \frac{1}{2}[1-\cos(\ell^2 qp\sin\phi)]$$
$$= \frac{1}{2}\int_0^{2\pi} \frac{d\phi}{2\pi} e^{\ell^2 qp\cos\phi}$$
$$- \frac{1}{2}\int_0^{2\pi} \frac{d\phi}{2\pi} e^{\ell^2 qp\cos\phi} \cos(\ell^2 qp\sin\phi). \tag{B2}$$

The two terms are evaluated separately. For the first term, one must note that[27]

$$e^{\ell^2 qp\cos\phi} = I_0(\ell^2 qp) + 2\sum_{n=1}^\infty I_n(\ell^2 qp)\cos(n\phi),$$

such that

$$\frac{1}{2}\int_0^{2\pi} \frac{d\phi}{2\pi} e^{\ell^2 qp\cos\phi} = \frac{1}{2} I_0(\ell^2 qp) \int_0^{2\pi} \frac{d\phi}{2\pi}$$
$$+ 2\sum_{n=1}^\infty I_n(\ell^2 qp) \frac{1}{2}\int_0^{2\pi} \frac{d\phi}{2\pi} \cos(n\phi)$$
$$= \frac{1}{2} I_0(\ell^2 qp). \tag{B3}$$

The second term

$$\frac{1}{2}\int_0^{2\pi} \frac{d\phi}{2\pi} e^{\ell^2 qp\cos\phi} \cos(\ell^2 qp\sin\phi)$$
$$= \frac{1}{2}\int_0^{2\pi} \frac{d\phi}{2\pi} \exp[\ell^2 qp\exp(i\phi)] = \frac{1}{2}. \tag{B4}$$

Substituting Eqs. (B3) and (B4) back into Eq. (B2) then yields the simpler expression,

$$\int_0^{2\pi} \frac{d\phi}{2\pi} e^{\ell^2 qp\cos\phi} \frac{1}{2}[1-\cos(\ell^2 qp\sin\phi)] = \frac{1}{2}[I_0(\ell^2 qp) - 1].$$

Now, substituting the above back into Eq. (B1) we find

$$\Sigma(p,\omega) = 4n_{\text{imp}}U^2 \int_0^\infty \frac{dq}{2\pi} q e^{-(\ell q)^2/2} e^{-(\ell p)^2/2} G(q,\omega)$$
$$\times \frac{1}{2}[I_0(\ell^2 qp) - 1]. \tag{B5}$$

APPENDIX C: BARE (LONG-WAVELENGTH) APPROXIMATION

To evaluate the self-energy within the long-wavelength approximation, we must return to Eq. (25). First, one remarks that the sine squared term in Eq. (25) greatly simplifies,

$$\sin^2\left(\frac{\mathbf{q}\wedge\mathbf{p}}{2}\right)\approx\left(\frac{\mathbf{q}\wedge\mathbf{p}}{2}\right)^2=\frac{1}{4}[\ell^2\hat{z}\cdot(\mathbf{q}\times\mathbf{p})]^2$$
$$=\frac{1}{4}(\ell^2|\mathbf{q}\times\mathbf{p}|)^2=\frac{1}{4}\ell^4|\mathbf{q}|^2|\mathbf{p}|^2\sin^2\phi. \tag{C1}$$

Then, substituting Eq. (C1) into Eq. (25) yields

$$\Sigma(\mathbf{p},\omega)=n_{\mathrm{imp}}U^2\ell^4\int_0^\infty\frac{dq}{2\pi}q^3e^{-(\ell q)^2/2}p^2e^{-(\ell p)^2/2}$$
$$\times G^0(\mathbf{q},\omega)\int_0^{2\pi}\frac{d\phi}{2\pi}e^{\ell^2pq\cos\phi}\sin^2\phi. \tag{C2}$$

The polar integral then turns out to match[27]

$$\int_0^{2\pi}\frac{d\phi}{2\pi}e^{\ell^2pq\cos\phi}\sin^2\phi=\frac{1}{2}[I_0(\ell^2pq)-I_2(\ell^2pq)]. \tag{C3}$$

The series expansion for Eq. (C3) gives ($x\equiv\ell^2pq$)

$$I_0(x)-I_2(x)=\left[1+\frac{x^2}{4}+\cdots\right]-\left[\frac{x^2}{8}+\cdots\right]=1+\frac{x^2}{8}+\cdots. \tag{C4}$$

Equation (C2) already holds a q^3p^2 term and therefore a q^5p^4 term is not needed in the long-wavelength approximation. Thus, one assumes that

$$I_0(\ell^2pq)-I_2(\ell^2pq)\approx 1. \tag{C5}$$

Moreover, the momenta are rescaled as $\mathbf{q},\mathbf{p}\to\mathbf{q}/\ell,\mathbf{p}/\ell$. As a result, Eq. (C2) simplifies to

$$\Sigma(p,\omega)=\frac{n_{\mathrm{imp}}U^2}{4\pi\ell^2}p^2e^{-p^2/2}\int_0^\infty dqq^3e^{-q^2/2}\frac{1}{\omega-\omega_q+i\eta},$$

where we replaced $G^0(\mathbf{q},\omega)$ by its definition [see Eq. (17)]. One can then make use of the identity[22]

$$\frac{1}{x+i\eta}=\mathcal{P}\frac{1}{x}-i\pi\delta(x), \tag{C6}$$

where $\mathcal{P}$ symbolizes the Cauchy principal value of the integral. Consequently, one has

$$\mathrm{Re}\,\Sigma(p,\omega)=\left(\frac{\epsilon_B}{4}\right)^2up^2e^{-p^2/2}\mathcal{P}\int_0^\infty dq\frac{q^3e^{-q^2/2}}{\omega-\omega_q}, \tag{C7}$$

$$\mathrm{Im}\,\Sigma(p,\omega)=-\left(\frac{\epsilon_B}{4}\right)^2up^2e^{-p^2/2}\int_0^\infty dqq^3e^{-q^2/2}\pi\delta(\omega-\omega_q). \tag{C8}$$

Let us first examine the real part of the self-energy, which actually denotes the physical self-energy.

It has been shown[12] that in the long-wavelength approximation the bosonic dispersion relation for $\mathbf{q}$ can be written as

$$\omega_{\mathbf{q}}=g+\frac{\epsilon_B}{4}q^2. \tag{C9}$$

The physical self-energy then becomes

$$\mathrm{Re}\,\Sigma(p,\omega)=\left(\frac{\epsilon_B}{4}\right)^2up^2e^{-p^2/2}\mathcal{P}\int_0^\infty dq\frac{q^3e^{-q^2/2}}{\omega-g-\frac{\epsilon_B}{4}q^2}. \tag{C10}$$

Let us then work temporarily with the new quantities

$$\bar{\omega}=\frac{4\omega}{\epsilon_B}\quad\text{and}\quad\bar{g}=\frac{4g}{\epsilon_B}, \tag{C11}$$

such that the self-energy is rewritten as

$$\mathrm{Re}\,\Sigma(p,\bar{\omega})=\frac{\epsilon_B}{4}up^2e^{-p^2/2}\mathcal{P}\int_0^\infty dq\frac{q^3e^{-q^2/2}}{\bar{\omega}-\bar{g}-q^2}.$$

Now, one performs a change in variable in the q momentum: $q\to\tilde{q}=q^2$. One must note that $qdq=d(q^2)/2$ and that the integration limits are not altered. Consequently, one gets

$$\mathrm{Re}\,\Sigma(p,\bar{\omega})=\frac{\epsilon_B}{4}up^2e^{-p^2/2}\mathcal{P}\int_0^\infty\frac{d\tilde{q}}{2}\frac{\tilde{q}e^{-\tilde{q}/2}}{\bar{\omega}-\bar{g}-\tilde{q}}. \tag{C12}$$

A further change in the integration variable is performed $\tilde{q}\to k=\bar{\omega}-\bar{g}-\tilde{q}$, leading to

$$\mathrm{Re}\,\Sigma(p,\bar{\omega}) = -\frac{\epsilon_B}{4}up^2e^{-p^2/2}\mathcal{P}\int_{\bar{\omega}-\bar{g}}^{-\infty}\frac{dk}{2}(\bar{\omega}-\bar{g}-k)e^{-(\bar{\omega}-\bar{g}-k)/2}\frac{1}{k}$$

$$= \frac{\epsilon_B}{4}up^2e^{-p^2/2}\Bigg[\left(\frac{\bar{\omega}-\bar{g}}{2}\right)\underbrace{\left(\mathcal{P}\int_{-\infty}^{\bar{\omega}-\bar{g}}d\left(\frac{k}{2}\right)\frac{e^{(k/2)}}{\left(\frac{k}{2}\right)}\right)}_{\textbf{Term a}}e^{-(\bar{\omega}-\bar{g})/2}$$

$$-\frac{1}{2}\underbrace{\left(\mathcal{P}\int_{-\infty}^{\bar{\omega}-\bar{g}}dkk\frac{e^{k/2}}{k}\right)}_{\textbf{Term b}}e^{-(\bar{\omega}-\bar{g})/2}\Bigg]. \tag{C13}$$

Term a corresponds to the definition of the exponential integral function;[27]

$$\mathrm{Ei}\left(\frac{\bar{\omega}-\bar{g}}{2}\right) = \mathcal{P}\int_{-\infty}^{\bar{\omega}-\bar{g}}d\left(\frac{k}{2}\right)\frac{e^{(k/2)}}{\left(\frac{k}{2}\right)}, \tag{C14}$$

whereas Term b can be straightforwardly integrated,

$$\mathcal{P}\int_{-\infty}^{\bar{\omega}-\bar{g}}dkk\frac{e^{k/2}}{k} = \int_{-\infty}^{0}d\tilde{k}e^{(\tilde{k}+\bar{\omega}-\bar{g})/2}$$

$$= \left(\int_{-\infty}^{0}d\tilde{k}e^{\tilde{k}}\right)e^{(\bar{\omega}-\bar{g})/2} = 2e^{(\bar{\omega}-\bar{g})/2}, \tag{C15}$$

where the shift of variable $k\rightarrow\tilde{k}=k-(\bar{\omega}-\bar{g})$ was used in the first step.

Thus, the physical self-energy becomes

$$\mathrm{Re}\,\Sigma(p,\bar{\omega}) = \frac{\epsilon_B}{4}up^2e^{-p^2/2}\Bigg[-1 + \left(\frac{\bar{\omega}-\bar{g}}{2}\right)\mathrm{Ei}\left(\frac{\bar{\omega}-\bar{g}}{2}\right)e^{-(\bar{\omega}-\bar{g})/2}\Bigg]. \tag{C16}$$

The renormalized energy of the bosons is obtained by looking at the poles of the full disorder self-averaged Green's function,

$$\omega-\omega_{\mathbf{p}}-\mathrm{Re}\,\Sigma(\mathbf{p},\omega) = 0. \tag{C17}$$

Consequently, in the long-wavelength approximation, the renormalized dispersion relation takes the form

$$\bar{\omega}-\bar{g} = p^2 + up^2e^{-p^2/2}\left[-1+\left(\frac{\bar{\omega}-\bar{g}}{2}\right)\mathrm{Ei}\left(\frac{\bar{\omega}-\bar{g}}{2}\right)e^{-(\bar{\omega}-\bar{g})/2}\right]. \tag{C18}$$

It is straightforward to notice that the renormalized spin stiffness, which corresponds to the coefficient of the p^2 term, is given by

$$\rho_s^R = \frac{\epsilon_B}{4}(1-u). \tag{C19}$$

We now turn to the imaginary part of the self-energy given by Eq. (C8). In the long-wavelength approximation, the Dirac delta function becomes

$$\delta(\omega-\omega_q) \approx \delta\left[\omega-\left(g+\frac{\epsilon_B}{4}q^2\right)\right] = \frac{4}{\epsilon_B}\delta(\bar{\omega}-\bar{g}-q^2). \tag{C20}$$

By performing a change in variable in the q momentum, $q\rightarrow\tilde{q}=q^2$ and replacing Eq. (C20) into Eq. (C8) one gets

$$\mathrm{Im}\,\Sigma(p,\bar{\omega}) = -\frac{\pi}{2}up^2e^{-p^2/2}(\omega-g)e^{-2(\omega-g)/\epsilon_B}. \tag{C21}$$

Finally, the scattering time, which amounts to the lifetime of the bosonic excitation, is given by

$$\frac{1}{\tau_{\mathbf{p}}} = \pi up^2e^{-p^2/2}(\omega-g)e^{-2(\omega-g)/\epsilon_B}. \tag{C22}$$

It is clear that $\tau_{\mathbf{p}}\rightarrow\infty$ when $\omega\rightarrow g$, i.e., low-energy quasiparticles are long lived, with finite lifetime induced by disorder.

APPENDIX D: PAULI SUSCEPTIBILITY

The Pauli susceptibility in case of linear response is given by the Kubo formula

$$\chi_{zz}(\mathbf{x},\mathbf{x}';t-t') = i\langle T_tS_z(\mathbf{x},t)S_z(\mathbf{x}',t')\rangle. \tag{D1}$$

Using the Fourier transformation

$$S_z(\mathbf{x},t) = \sum_{\mathbf{q}}S_z(\mathbf{q},t)e^{i\mathbf{q}\cdot\mathbf{x}}, \tag{D2}$$

the susceptibility can be written as

$$\chi_{zz}(\mathbf{q},\mathbf{q}';t-t') = i\langle T_tS_z(\mathbf{q},t)S_z(\mathbf{q}',t')\rangle. \tag{D3}$$

On the other hand, the operators $S_z(\mathbf{q},t)$ can be written in the bosonized form[12]

$$S_z(\mathbf{q},t) = \frac{N_\phi}{2}\delta_{\mathbf{q},0} - e^{-\mathbf{q}^2/4}\sum_{\mathbf{p}} \cos\left(\frac{\mathbf{q}\wedge\mathbf{p}}{2}\right) b^\dagger_{\mathbf{q}+\mathbf{p}}(t) b_{\mathbf{p}}(t),$$

where $b_{\mathbf{p}}(t) = e^{iHt} b_{\mathbf{p}} e^{-iHt}$. Thus, after substitution

$$\chi_{zz}(\mathbf{q},\mathbf{q}';t-t') = ie^{-\mathbf{q}^2/2}\sum_{\mathbf{p},\mathbf{p}'} \cos\left(\frac{\mathbf{q}\wedge\mathbf{p}}{2}\right)\cos\left(\frac{\mathbf{q}\wedge\mathbf{p}'}{2}\right) \times \langle T_t b^\dagger_{\mathbf{q}+\mathbf{p}}(t) b_{\mathbf{p}}(t) b^\dagger_{\mathbf{q}'+\mathbf{p}'}(t') b_{\mathbf{p}'}(t')\rangle.$$

Evaluation of the expectation value yields

$$\chi_{zz}(\mathbf{q},\mathbf{q}';t-t') = -ie^{-\mathbf{q}^2/2}\sum_{\mathbf{p},\mathbf{p}'} \cos\left(\frac{\mathbf{q}\wedge\mathbf{p}}{2}\right)\cos\left(\frac{\mathbf{q}\wedge\mathbf{p}'}{2}\right) \times G(\mathbf{p}'+\mathbf{q}',\mathbf{p};t-t')G(\mathbf{p}+\mathbf{q},\mathbf{p}';t'-t),$$

using the notation defined earlier in Eq. (12). Expanding the Green's function $G(\mathbf{p},\mathbf{q};t-t')$ into the Born series and performing the disorder averaging one recovers the translational invariance $\langle\chi_{zz}(\mathbf{q},\mathbf{q}';t-t')\rangle_{\text{imp}} = \delta_{\mathbf{q}+\mathbf{q}',0}\chi_{zz}(\mathbf{q},t-t')$. Moreover, performing the Fourier transformation in the time variable t and introducing

$$P(\mathbf{p},\mathbf{q};\omega,\epsilon) \equiv \sum_{\mathbf{p}'} \cos\left(\frac{\mathbf{q}\wedge\mathbf{p}'}{2}\right) \times \langle G(\mathbf{p}'-\mathbf{q},\mathbf{p};\omega+\epsilon)G(\mathbf{p}+\mathbf{q},\mathbf{p}';\omega)\rangle_{\text{imp}}$$

the susceptibility is

$$\chi_{zz}(\mathbf{q},\epsilon) = \frac{-iAe^{-\mathbf{q}^2/2}}{(2\pi)^3}\int d\mathbf{p}\int_{-\infty}^{\infty} d\omega \cos\left(\frac{\mathbf{q}\wedge\mathbf{p}}{2}\right) P(\mathbf{p},\mathbf{q};\omega,\epsilon). \tag{D4}$$

In the self-consistent approximation the function $P(\mathbf{p},\mathbf{p}';\omega,\epsilon)$ obeys[22]

$$P(\mathbf{p},\mathbf{p}';\omega,\epsilon) = G(\mathbf{p},\omega+\epsilon)G(\mathbf{p}+\mathbf{p}',\omega)\left[\cos\left(\frac{\mathbf{p}\wedge\mathbf{p}'}{2}\right) + \frac{AN_{\text{imp}}}{(2\pi)^2}\int d\mathbf{q}U^e(\mathbf{p}-\mathbf{q},\mathbf{q}) \times U^e(\mathbf{q}-\mathbf{p},\mathbf{p}+\mathbf{p}')P(\mathbf{q},\mathbf{p}';\omega,\epsilon)\right].$$

We are interested mostly in the static susceptibility $\chi \equiv \lim_{\epsilon\to 0}\chi_{zz}(0,\epsilon)$. Thus, in particular

$$P(\mathbf{p},0;\omega,0) = G^2(\mathbf{p},\omega)\left[1 + \frac{AN_{\text{imp}}}{(2\pi)^2}\int d\mathbf{q}U^e(\mathbf{p}-\mathbf{q},\mathbf{q}) \times U^e(\mathbf{q}-\mathbf{p},\mathbf{p})P(\mathbf{q},0;\omega,0)\right].$$

A spherically symmetric solution satisfies

$$P(p,0;\omega,0) = G^2(p,\omega)\left\{1 + \frac{u}{4}\epsilon_B^2 e^{-p^2/2}\int_0^\infty dqqe^{-q^2/2} \times [I_0(qp)-1]P(q,0;\omega,0)\right\}. \tag{D5}$$

Let us introduce a new function

$$H(p,\omega) \equiv P(p,0;\omega,0)G^{-2}(p,\omega); \tag{D6}$$

then Eq. (D5) can be rewritten as

$$H(p,\omega) = 1 + \frac{u}{4}\epsilon_B^2 e^{-p^2/2}\int_0^\infty dqqe^{-q^2/2} \times [I_0(qp)-1]G^2(q,\omega)H(q,\omega), \tag{D7}$$

or explicitly

$$H(p,\omega) = 1 + \frac{u}{4}\epsilon_B^2 e^{-p^2/2}\int_0^\infty dqqe^{-q^2/2} \times \frac{I_0(qp)-1}{[\omega-\omega_q-\Sigma_u(q,\omega)]^2}H(q,\omega). \tag{D8}$$

Notice that Eq. (D8) has the same form as Eq. (46) but with $H(p,\omega)$ instead of $\partial_u\Sigma_u(p,\omega)$, which is known to diverge $\partial_u\Sigma_u(p,0)\to\infty$ when $u\to u_c$. In the next part we will demonstrate that $H(p,0)$ also diverges, $H(p,0)\to\infty$ when $u\to u_c$.

We are looking for a solution in the form

$$H(p,\omega) = 1 + e^{-p^2/2}\sum_{n=1}^{\infty} h_n(\omega)p^{2n}, \tag{D9}$$

Substitution of Eq. (D9) into Eq. (D8) yields an expression, which looks similar to the equation previously obtained [see Eq. (49)],

$$h_n(\omega) = \frac{uK_n}{4(2^n n!)^2} + \frac{u}{4(2^n n!)^2}\sum_{k=1}^{\infty} F_{n+k}h_k(\omega), \tag{D10}$$

where the function F_n was defined earlier by Eq. (48) and

$$K_n \equiv \epsilon_B^2\int_0^\infty dq\frac{q^{2n+1}e^{-q^2/2}}{[\omega-\omega_q-\Sigma_u(q,\omega)]^2}. \tag{D11}$$

Notice that

$$K_n = \sum_{k=0}^{\infty}\frac{1}{2^k k!}F_{k+n} \tag{D12}$$

and

$$F_n = \sum_{k=0}^{\infty}\frac{(-1)^k}{2^k k!}K_{k+n}. \tag{D13}$$

Equivalently

$$\sum_{k=1}^{\infty} B_{n,k}2^k k!\, h_k(\omega) = \frac{uK_n}{2^{n+2}n!}, \tag{D14}$$

where $B_{n,k}$ was defined in Eq. (50). The solution is found by computing the inverse matrix to Eq. (D14) and has the form

$$h_n(\omega) = \frac{2^{-n}u}{4n!}\sum_{k=1}^{\infty} B^{-1}_{n,k}\frac{K_k}{2^k k!}. \tag{D15}$$

Therefore,

$$P(p,0;\omega,0) = G^2(p,\omega)\left(1 + e^{-p^2/2}\sum_{n=1}^{\infty} p^{2n}\frac{2^{-n}u}{4n!}\sum_{k=1}^{\infty} B^{-1}_{n,k}\frac{K_k}{2^k k!}\right) \tag{D16}$$

and

$$\int_0^\infty P(p,0;\omega,0)pdp = \int_0^\infty G^2(p,\omega)pdp + \sum_{n=1}^{\infty}\int_0^\infty e^{-p^2/2}p^{2n+1}G^2(p,\omega)dp\frac{2^{-n}u}{4n!}\sum_{k=1}^{\infty} B^{-1}_{n,k}\frac{K_k}{2^k k!}, \tag{D17}$$

if the integral is convergent. Otherwise, it has to be regularized, which we would not consider here. This leads to

$$\int_0^\infty P(p,0;\omega,0)pdp = \sum_{n=1}^{\infty}\frac{K_n}{2^n n!} + \frac{u}{4}\sum_{n,k=1}^{\infty}\frac{K_n}{2^n n!}B^{-1}_{n,k}\frac{K_k}{2^k k!}, \tag{D18}$$

which can be further simplified by means of some algebraic transformations,

$$\int_0^\infty P(p,0;\omega,0)pdp = F_0 + \sum_{n,k=1}^{\infty}\left[\frac{4}{u}(B^{-1}_{n,k} - \delta_{n,k}) + 2B^{-1}_{n,k}\frac{F_k}{2^k k!} + \frac{u}{4}\frac{F_n}{2^n n!}B^{-1}_{n,k}\frac{F_k}{2^k k!}\right]. \tag{D19}$$

Despite the simplifications, the above expression is difficult to evaluate analytically, as well as numerically. However, since most of the terms there involve the inverse matrix, it is reasonable to suppose that if $\omega=0$ it diverges with $u \to u_c$ as

$$\int_0^\infty P(p,0;0,0)pdp \sim \det[B(u)]^{-1}. \tag{D20}$$

On the other hand the susceptibility is given by

$$\chi(\epsilon) = -\frac{iA}{(2\pi)^2}\int_{-\infty}^{\infty} d\omega \int_0^\infty P(p,0;\omega,\epsilon)pdp. \tag{D21}$$

Thus, considering $\epsilon=0$, we see that the integrand is divergent at $\omega=0$ with $u \to u_c$, which can be considered as a possible indication of divergent Pauli susceptibility.

[1] A. G. Green, Phys. Rev. B **57**, R9373 (1998).
[2] J. Sinova, A. H. MacDonald, and S. M. Girvin, Phys. Rev. B **62**, 13579 (2000).
[3] S. Rapsch, J. T. Chalker, and D. K. K. Lee, Phys. Rev. Lett. **88**, 036801 (2002); D. K. K. Lee, S. Rapsch, and J. T. Chalker, Phys. Rev. B **67**, 195322 (2003).
[4] I. S. Burmistrov, JETP **95**, 132 (2002).
[5] J. Tomonaga, Prog. Theor. Phys. **5**, 544 (1950).
[6] A. Luther, Phys. Rev. B **19**, 320 (1979).
[7] F. D. M. Haldane, Helv. Phys. Acta **65**, 152 (1992).
[8] A. H. Castro Neto and E. Fradkin, Phys. Rev. B **49**, 10877 (1994).
[9] A. Houghton and J. B. Marston, Phys. Rev. B **48**, 7790 (1993).
[10] H. J. Kwon, A. Houghton, and J. B. Marston, Phys. Rev. B **52**, 8002 (1995).
[11] H. Westfahl, Jr., A. H. Castro Neto, and A. O. Caldeira, Phys. Rev. B **55**, R7347 (1997).
[12] R. L. Doretto, A. O. Caldeira, and S. M. Girvin, Phys. Rev. B **71**, 045339 (2005).
[13] O. Tieleman, A. Lazarides, D. Makogon, and C. Morais Smith, Phys. Rev. B **80**, 205315 (2009).
[14] Yu. A. Bychkov, S. V. Iordanskii, and G. M. Eliashberg, Pis'ma Zh. Eksp. Teor. Fiz. **33**, 152 (1981) [JETP Lett. **33**, 143 (1981)].
[15] C. Kallin and B. I. Halperin, Phys. Rev. B **30**, 5655 (1984).
[16] S. M. Girvin, A. H. MacDonald, and P. M. Platzman, Phys. Rev. B **33**, 2481 (1986).
[17] M. M. Fogler and B. I. Shklovskii, Phys. Rev. B **52**, 17366 (1995).
[18] E. F. Shender, J. Phys. C **11**, L423 (1978).
[19] I. Avgin, D. L. Huber, and W. Y. Ching, Phys. Rev. B **48**, 16109 (1993).
[20] A. H. MacDonald, P. M. Platzman, and G. S. Boebinger, Phys. Rev. Lett. **65**, 775 (1990).
[21] G. Murthy, Phys. Rev. B **64**, 241309(R) (2001).
[22] H. Doniach and E. H. Sondheimer, *Green's Functions for Solid State Physicists* (W. A. Benjamin, Reading, MA, 1974).
[23] R. L. Doretto (private communication).
[24] H. Bruus and K. Flensberg, *Many-Body Quantum Theory in Condensed-Matter Physics* (Oxford University Press, New York, 2006).
[25] A. A. Abrikosov, L. P. Gorkov, and I. E. Dzyaloshinski, *Methods of Quantum Field Theory in Statistical Physics* (Pergamon, New York, 1965).
[26] H. A. Fertig and G. Murthy, Phys. Rev. Lett. **95**, 156802 (2005).
[27] I. S. Gradshteyn and I. M. Ryzhik, *Table of Integrals, Series, and Products* (Academic, San Diego, 1994).